

# Anomalous enhancements of low-energy fusion rates in plasmas: the role of ion momentum distributions and inhomogeneous screening

M. Coraddu<sup>1,\*</sup>, Marcello Lissia<sup>1,2,§</sup>, P. Quarati<sup>1,3,4‡</sup>

<sup>1</sup>*Istituto Nazionale di Fisica Nucleare (INFN), Sezione di Cagliari, I-09042, Monserrato, Italy*

<sup>2</sup>*Dipart. di Fisica dell'Università di Cagliari, Cittadella universitaria, I-09042 Monserrato, Italy*

<sup>3</sup>*Dipartimento di Fisica - Politecnico di Torino, I-10129, Italy*

<sup>4</sup>*Istituto Nazionale per la Fisica della Materia (CNR-INFN), Sezione del Politecnico di Torino, I-10129, Italy*

Non-resonant fusion cross-sections significantly higher than corresponding theoretical predictions are observed in low-energy experiments with deuterated matrix target. Models based on thermal effects, electron screening, or quantum-effect dispersion relations have been proposed to explain these anomalous results: none of them appears to satisfactorily reproduce the experiments. Velocity distributions are fundamental for the reaction rates and deviations from the Maxwellian limit could play a central role in explaining the enhancement. We examine two effects: an increase of the tail of the target Deuteron momentum distribution due to the Galitskii-Yakimets quantum uncertainty effect, which broadens the energy-momentum relation; and spatial fluctuations of the Debye-Hückel radius leading to an effective increase of electron screening. Either effect leads to larger reaction rates especially large at energies below a few keV, reducing the discrepancy between observations and theoretical expectations.

Keywords: Kinetic theory Fusion reactions Particles measurements

## 1. INTRODUCTION

In the last ten years a number of different experiments with target Deuterons absorbed in a metallic matrix have found strong enhancements of fusion reaction rates below a few keV. The fusion of the implanted Deuterons with the incoming ions ( $D^+$  or  $Li^+$ ) has been observed; the  $d(d,t)p$  reaction has been investigated in refs. [1, 2, 3, 4, 5, 6, 7, 8, 9, 10, 11] and the  ${}^6,7Li(d,\alpha){}^4,5He$  reactions have been studied in refs. [12, 13, 14, 15] finding similar strong enhancements. Experiments with gas targets show much weaker enhancements, which can be explained by standard electron screening with a potential  $U_e$  of the same order of the adiabatic limit  $U_{ad} = 28$  eV. In other words, the penetration through a screened Coulomb barrier at energy  $E$  is equivalent to that of bare nuclei at energy  $E + U_e$ . The adiabatic limit is reached when the correspondent enhancement of nuclear cross section can be explained by the gain of the electron binding energies  $U_{ad}$  between the initial distant atoms and the final fused nuclei setting  $U_e = U_{ad}$  [16].

The same type of screening mechanism could reproduce results for deuterated metal target experiments only using an unreasonable large potential  $U_e$  of hundreds of eV, ten times greater than the adiabatic limit  $U_{ad}$ .

A tentative explanation [8, 9, 10, 11], based on a simplified model of the classical quasi-free electrons, needs an electron screening distance of the order of the Debye length. This approach reproduces both the correct size of the screening potential  $U_e$  and its dependence on the temperature:  $U_e \propto T^{1/2}$  [8, 10]. However, this model lacks a clear physical interpretation such as the one for the Debye screening, which is a cooperative effect, since the mean-number of quasi-free particles in the Debye sphere [17] is much smaller than one.

The thermal motion of the target atoms is another mechanism capable of increasing the reaction rate; however, Maxwellian momentum distribution at the experimental temperatures gives negligible effects [18, 19]. The relationship

between energy and momentum of quasi particles can be broadened by many-body collisions [20], then even a Maxwell-Boltzmann energy distribution leads to a momentum distribution with an enhanced power-law tail. Fusion processes select high-momentum particles that are able to penetrate the Coulomb barrier and are, therefore, extremely sensitive probes of the distribution tail [21, 22, 23, 24, 25]. This Quantum Uncertainty Effect has been proposed in [19, 24, 26, 27, 28, 29] as a possible contribution to the reaction rate enhancements.

These two mechanisms clearly cannot take into account all the complex many-body physics in plasmas. In different contexts other approaches exist both to fluctuations and to strong-coupled screening [16].

Among the over 50 different targets (metals and insulators) where deuteron fusion reactions have been studied, this present work focuses on the paradigmatic case of Ta matrix to show how either of the two effects we consider reduces the discrepancy between theoretical predictions and experimental data. This case has been extensively studied by different experimental groups and there exist many published data [3, 4, 5, 6, 7, 8] in reasonable agreement. Both effects yield qualitatively similar results when applied to other targets, but detailed quantitative comparisons need further work.

We review the experimental procedure in section 2 and evaluate the consequence of the Quantum Uncertainty Effect in section 3. The plasma screening effects on the reaction rate are evaluated in section 4, using for the first time the modified Debye-Hückel potential proposed by Quarati and Scarfone in ref. [30], which is an approach introduced to study deviations from the weakly coupled plasma limit, where the standard Debye-Hückel screening applies. We draw our conclusions in section 5.

## 2. EXPERIMENTAL PROCEDURE

All experiments performed to investigate the  $D + D \rightarrow T + p$  fusion reaction, in all different target matrices, employ a Deuterons ion beam of energy  $1 \text{ keV} \leq E_b \leq 100 \text{ keV}$ , that is totally absorbed by the thin foil ( $\sim 0.1 \text{ mm}$ ) of deuterated target, at room temperature of about  $10^\circ\text{C}$ . Detectors count the total number  $N(E_b, \theta)$  of fusion reaction protons emitted in  $\theta$  directions, and the results can be expressed in terms of the reaction Yield of an infinitely thick target:  $Y_{exp}^\infty = N(E_b, \theta)/N_p$ , where  $N_p$  is the total number of incident projectiles.

If we consider the target nuclei at rest, the thick target reaction Yield can be expressed as:

$$Y_{th}^\infty(E_b, \theta) = \varepsilon n_D \int_0^{E_b} \sigma(E) \left( \frac{dE}{dx} \right)^{-1} dE, \quad (2.1)$$

where  $n_D$  is the density of the target deuterons,  $\varepsilon$  is the proton detection efficiency,  $\sigma(E)$  is the fusion cross section and  $(\frac{dE}{dx})$  is the energy loss for unit length, or Stopping Power. The effect of the thermal motion of target deuterons modifies  $Y_{th}^\infty$  in:

$$Y_{th}^\infty(E_b, \theta) = \varepsilon n_D \int_0^{E_b} \frac{\langle \sigma v_{rel} \rangle}{v} \left( \frac{dE}{dx} \right)^{-1} dE, \quad (2.2)$$

where  $v_{rel} = |\mathbf{v} - \mathbf{v}_t|$  is the relative velocity,  $v_t$  and  $v = \sqrt{2E/m_D}$  are the target and the incident particle velocities,  $E$  is the incident deuteron energy inside the target,  $m_D$  is the deuteron mass, and  $\langle \sigma v_{rel} \rangle = \int d^3\mathbf{p}_t \Phi(\mathbf{p}_t) \sigma v_{rel}$  is the thermal mean with  $\Phi(\mathbf{p}_t)$  the distribution of particle momentum target  $\mathbf{p}_t$ . For the Stopping Power  $(\frac{dE}{dx})$  all the authors adopt the values reported by Andersen and Ziegler [31].

In the zero-temperature approximation the reaction cross section  $\sigma_{exp}(E)$  can be extracted from  $Y_{exp}^\infty$  through a finite-interval numeric differentiation:

$\sigma_{exp} = \frac{(\frac{dE}{dx})}{\varepsilon n_D} \frac{Y_{exp}^\infty(E_b, \vartheta) - Y_{exp}^\infty(E_b - \Delta E_b, \vartheta)}{\Delta E_b}$ , where  $\Delta E_b$  is a small beam energy step between two subsequent measurements of  $Y_{exp}^\infty$ . If thermal effects are included, this procedure yields  $(\langle \sigma v_{rel} \rangle / v)_{exp}$  instead of  $\sigma_{exp}$ . A convenient theoretical expression for the bare-nucleus cross section is:

$$\sigma_{th}(E_{cm}) = \frac{S(E_{cm})}{E_{cm}} \exp \left[ -\pi \sqrt{\frac{E_G}{E_{cm}}} \right], \quad (2.3)$$

where the exponential factor is the penetration function across the bare repulsive Coulomb potential,  $E_G = 2\mu Z_1^2 Z_2^2 e^4 / \hbar^2$  is the Gamow energy,  $\mu$  is the reduced mass  $Z_1, Z_2$  are the atomic numbers of the interacting nuclei and  $S(E_{cm})$  is the astrophysical factor. If the small thermal effects are neglected, the center of mass energy is  $E_{cm} = E_b/2$ . Static electron screening can be taken into account by introducing the electron screening potential  $U_e$ :

$$\sigma_{th}(E_{cm}) = \frac{S(E_{cm})}{E_{cm} + U_e} \exp \left[ -\pi \sqrt{\frac{E_G}{E_{cm} + U_e}} \right]. \quad (2.4)$$

Theoretical calculations and experimental results are often conveniently reported in terms of the Astrophysical Factor  $S(E)$ :  $S_{th,exp}(E_{cm}) = E_{cm} \exp \left[ \pi \sqrt{\frac{E_G}{E_{cm} + U_e}} \right] \sigma_{th,exp}$ , since

it depends much less strongly on energy. Of course, while  $S_{exp}(E_{cm})$  is extracted from  $Y_{exp}^\infty$ , the quantity  $S_{th}(E_{cm})$  depends on the value of  $U_e$  and on the theoretical cross section.  $S_{th}(E_{cm})$  would in principle include all many-body effects, which modify the bare cross section in vacuum. In this work we consider, separately, only two effects as dominant for the reaction rate: the quantum broadening effect on the momentum distribution and the electron screening, which we evaluate beyond the Debye-Hückel approximation given the plasma density inside the metal matrix. The case of Deuterated Tantalum target has been investigated extensively [3, 4, 5, 6, 7, 8]. Measurements are reported with great detail in ref. [6], then we adopt the relative experimental environment for our comparison: matrix target chemical composition is pure Ta ( $Z = 73$ ,  $A = 180.948 \text{ a.m.u.}$ ), target temperature  $T = 10^\circ\text{C}$ , Ta density at room temperature  $\rho = 16.65 \text{ g cm}^{-3}$  ( $n_{Ta} = 5.54 \cdot 10^{22} \text{ cm}^{-3}$ ), stoichiometric coefficient  $x = 7.9$ , absorbed Deuterium density  $n_D = 0.701 \cdot 10^{22} \text{ cm}^{-3}$ . Fig. 1 shows both  $Y_{exp}^\infty$  and the extracted  $S_{exp}$ , relative to the deuterated Tantalum experiment of ref. [6]. The experimental results can be reproduced only with an electron screening potential  $U_e = 309 \text{ eV} \gg U_{ad} = 28 \text{ eV}$ ; similar large screening potentials are needed to fit other deuterated-Tantalum experiments:  $U_e = 322 \text{ eV}$  in ref. [3] and  $U_e = 340 \text{ eV}$  in ref. [7, 8]. The experimental procedure has been critically studied in [4, 5], especially target surface contaminations and inhomogeneities in the implanted deuterons distribution have been identified as possible sources of systematic errors in the experimental data. However, performing deuterated Tantalum targets experiments with different surface contaminations, the electron screening potential needed to reproduce the data is in the range  $U_e = 210 - 460 \text{ eV}$  [4, 5], much greater than  $U_{ad}$  and in agreement with the previous results. In the absence of incoming beam there are ions and conduction electrons inside the metallic matrix, while the ion beam may ionize deuteron atom target or metallic ions, so additional charges may appear. Accurate numerical simulations performed by Huke et al. [32] suggest migration of electrons from the host metal atoms to the Hydrogen ions during the impact event. This effect produces a screening potential  $U_e = 39.7 \text{ eV}$  for deuterated-Tantalum target, greater than  $U_{ad}$  but still one order of magnitude lower than the one needed to explain the experimental results.

## 3. THERMAL EFFECTS AND QUANTUM UNCERTAINTY.

Collision frequency among target and incoming deuterons is the most important quantity to consider in this treatment. Collision frequencies among other particles, e.g., target atoms and metallic ions, are less important and are not responsible of modification of momentum distribution function and of fusion rate [33]. Momentum-energy dispersion relation is broadened by Quantum Uncertainty Effect (QE), so that a Maxwell-Boltzmann energy distribution  $\Phi(E) \propto \exp(-E/k_b T)$  can yield corresponding momentum distributions  $\Phi(\mathbf{p}_t)$  with enhanced tails. Since nuclear fusion cross section depends on

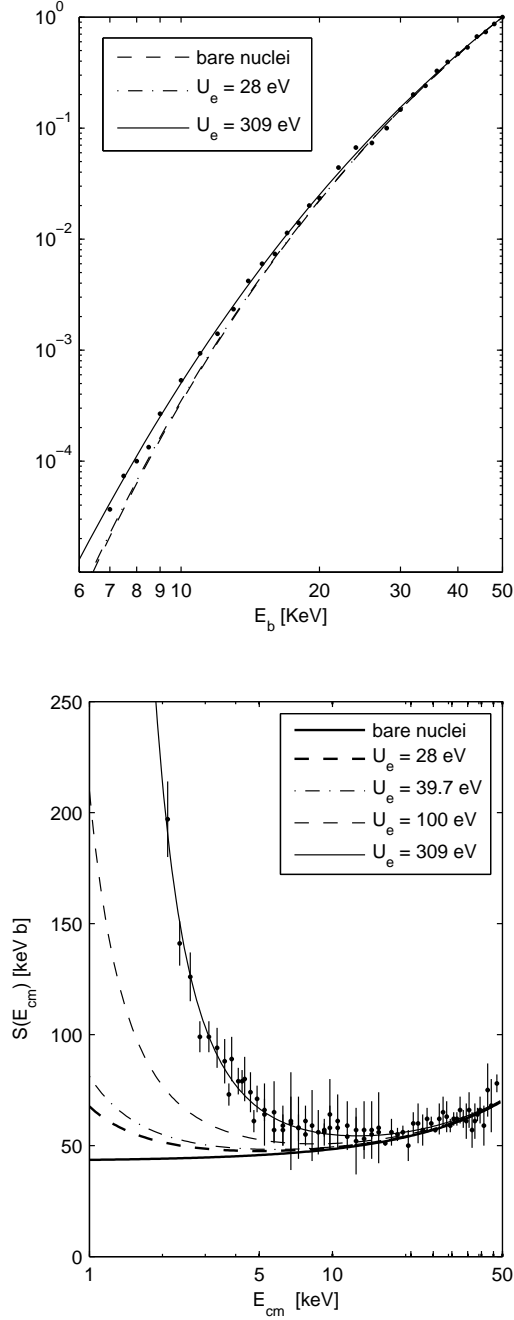


FIG. 1: Experimental results from ref. [6]. Upper panel:  $Y_{th}^{\infty}$  data points from one of the 13 runs weighted to extract the cross section  $\sigma_{exp}$ ; data normalized to a beam energy  $E_b$  (Lab frame) of 50 keV;  $Y_{th}^{\infty}$  curves from eq. (2.1) are computed with eq. (2.3) (bare) and eq. (2.4) (screened) cross sections. Lower panel: Astrophysical Factor data points  $S_{exp}$  extracted from  $Y_{exp}^{\infty}$ ; bare Astrophysical Factor is assumed to be  $S(E_{cm}) = 43 + 0.54 E_{cm}$  keV b, by normalization with higher energy results ( $E_{cm} \geq 40$  keV), while screened  $S_{th}$  curves are obtained from eq. (2.4). Thermal effect are neglected.

the relative momentum  $\epsilon_{p_{rel}} = \frac{1}{2}\mu v_{rel}$  such an effect increases the value of  $\langle \sigma(\epsilon_{p_{rel}}) v_{rel} \rangle / v$  respect to the one obtained with a sharp energy-momentum relation. It is a good approximation of the experimental situation to consider a beam of particles with definite energy and momentum and a Maxwell-Boltzmann energy distribution of thermalized target particles. The momentum-energy relation of the target particle can be represented with a Lorentzian [20], at least for  $E_t \sim \epsilon_p$ :

$$\delta_{\gamma}(E_t - \epsilon_{p_t}) = \frac{1}{\pi} \frac{\gamma}{(E_t - \epsilon_{p_t})^2 + \gamma^2}, \quad (3.1)$$

where  $\epsilon_{p_t} = \frac{1}{2}m_D v_t^2$ ,  $\gamma = \hbar n_D \sigma_{coll} v_{coll}$ ,  $\sigma_{coll}$  and  $v_{coll} = \sqrt{2E_t/m_D}$  are the collisional cross section and velocity. In [19, 24, 26, 27] Quantum Uncertainty Effect has been applied to the fusion reaction between beam and absorbed deuterons, adopting a Coulombian collisional cross section  $\sigma_{coll} = e^4/\epsilon_{p_t}^2$ . This QE produces a rate increase, but only at beam energies lower than the energy at which the experimental results start rising ( $E_b \sim 2$  keV for ref. [6] instead of  $E_b \sim 6 - 8$  keV, as shown in fig. 2).

Zubarev [28, 29] proposes that the QE should be effective only for a small fraction of target deuterons that are in a quasi-free mobile plasma states in the reaction zone and that the rate enhancement is due to reactions of deuterons of this small plasma fraction with the other stationary deuterons in the target. The beam is only needed to maintain the plasma states. Zubarev reproduces the enhancement with this mechanism and a Coulombian collisional cross section.

However, collisional cross sections depend on the plasma environment. In particular, the Coulombian cross section  $\sigma_{coll} = e^4/\epsilon_{p_t}^2$  is appropriate only for weakly interacting plasmas, i.e., plasmas with parameter  $\Gamma = \frac{e^2}{k_b T a_{ws}} \ll 1$ , where  $a_{ws} = (3/4\pi n_D)^{1/3}$  is the Wigner-Seitz radius, but  $\Gamma \sim 100$  for the typical experimental conditions we are interested in, see for instance ref. [6], where  $n_D = 0.701 \cdot 10^{22} \text{ cm}^{-3}$ ,  $k_b T = 0.0244 \text{ eV}$ ,  $a_{ws} = 3.24 \cdot 10^{-8} \text{ cm}$ , resulting in  $\Gamma = 182$  (very close to the liquid-solid transition). Therefore, a strong coupled plasma scheme should be used for the absorbed deuterons. A model that can describe the screened collisional cross section in this limit is the Ion Sphere Model [17]:

$$\sigma_{coll} = 2\pi\alpha_1^2 a_{ws}^2. \quad (3.2)$$

Eq. 3.2 is a non trivial expression for  $\sigma_{coll}$ , because the parameter  $\alpha_1$  contains information on the particle-particle correlations and in ref.s [34, 35] (and citation therein) Ichimaru and collaborators have given a detailed analysis of its expression and evaluation. For what concerns the present problem we can say that  $\alpha_1$  is a correlation factor of the order of unity or, more precisely, that its value lies between 0.4 and 0.9.

The resulting distribution for  $\mathbf{p}_t$  is  $\Phi(\mathbf{p}_t) = \frac{1}{I_N} \int_0^\infty dE_t \delta_{\gamma}(E_t - \epsilon_{p_t}) e^{-E_t/k_b T}$ , where  $I_N = 4\pi \int_0^\infty p_t^2 dp_t \int_0^\infty dE_t \delta_{\gamma}(E_t - \epsilon_{p_t}) e^{-E_t/k_b T}$  is the normalization

integral. Therefore, the thermal mean is:

$$\begin{aligned} \langle \sigma v_{rel} \rangle_{QE} &= \int d^3 \mathbf{p}_t \Phi(\mathbf{p}_t) \sigma v_{rel} = \frac{2\pi m_D^{2/3}}{I_N} \int_{-1}^{+1} d \cos \vartheta \\ &= \int_0^\infty d\varepsilon_{p_t} \sqrt{2\varepsilon_{p_t}} \int_0^\infty dE_t \delta_\gamma(E_t - \varepsilon_{p_t}) e^{-E_t/k_b T} \sigma(\varepsilon_{p_{rel}}) v_{rel}, \end{aligned} \quad (3.3)$$

where  $\vartheta$  is the angle between  $\mathbf{p}_t$  and the beam and  $v_{rel} = \sqrt{2/m_D} (E_b + \varepsilon_{p_t} - 2\sqrt{E\varepsilon_{p_t}} \cos \vartheta)^{1/2}$ .

Eq. (3.3) has been numerically evaluated with parameters appropriate to the experiment of ref. [6] using a constant Astrophysical factor  $S(\varepsilon_{p_{rel}}) \simeq S_0 = 43 \text{ keV b}$ , valid within  $\approx 6\%$  for  $E_b \leq 10 \text{ keV}$ . The  $\vartheta$  integration has been done analytically in terms of incomplete Gamma-Euler function, while the remaining integrations have been performed using the Gauss adaptive method; results are shown in fig. 2 for Coulombian and Ion Sphere Model (ISM) collisional cross sections. Both cases yield a strong enhancement of the reaction rates at low-energy: below  $E_b \sim 2 \text{ keV}$  for the Coulombian and below  $E_b \sim 10 \text{ keV}$  for the ISM case. These behaviors should be compared to the anomalous enhancement of the experimental data that start below energies  $E_b \sim 4 - 6 \text{ keV}$ . In the ISM case, the energy-threshold below which the rate is enhanced depends on  $\sigma_{coll}$  that, in turns, depends on  $n_D^{-2/3}$ , (see eq. (3.2)). Our calculation uses no adjustable parameter ( $\alpha_1 = 1$  in fig. 2), however, if we follow the approach of Kim and Zubarev in ref. [29], we could apply the enhancement only to that fraction of the absorbed deuterons that is in a quasi-free plasma state. The dependence of the reaction rate  $r$  on the fraction  $f = n_{D_m}/n_D$  of absorbed target Deuterons,  $n_D$ , that are quasi-free,  $n_{D_m}$ , is not trivial:  $r$  is not simply proportional to  $f$ , but it has an additional dependence on  $f$  through the ISM collisional cross section  $\sigma_{coll}$  eq. (3.2); it is clear, however, that  $f = 1$  gives the maximal effect. In principle, the fraction  $f$  could be calculated in some theoretical model, determined from an independent experimental measurement, or used as a free parameter to be fitted. Results presented have been obtained with  $f = 1$  and, therefore, should be interpreted as upper limits for this effect.

#### 4. MODIFIED DEBYE-HÜCKEL SCREENING.

We discuss the effect of electron screening on deuteron-fusion reactions in metal matrix. We do not consider the interplay with the effect discussed in the previous section. The screening potential at distances near and below the turning point influence the most reaction rates. Thermal effects and screening phenomena in plasma environment are strictly connected. Assuming, in a ideal plasma, a Maxwell-Boltzmann (M-B) thermal distribution, the Debye-Hückel ion-screening potential  $V_{DH}(r) = \frac{Z_1 Z_2 e^2}{r} \exp(-r/R_{DH})$  is obtained by means of the linear Poisson equation ( $R_{DH} = \sqrt{k_b T / 4\pi n Z e^2}$  is the Debye-Hückel radius). In strongly coupled plasmas, Debye description loses its physical interpretation. In the case studied, the main reason is that the number of particles inside the

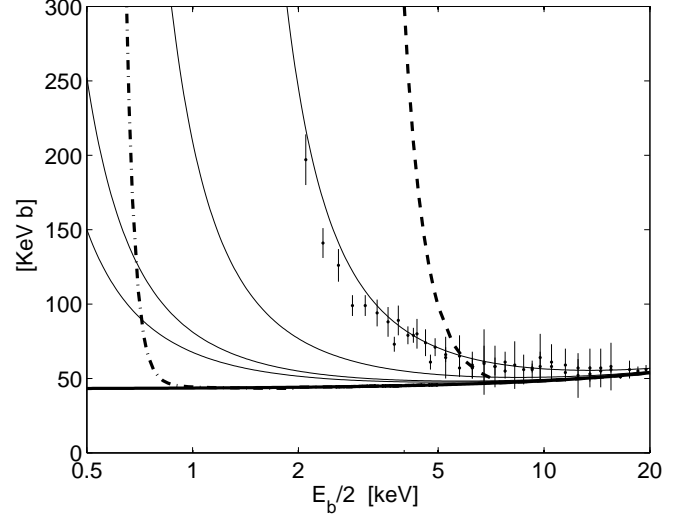


FIG. 2: Astrophysical Factor experimental points from ref. [6];  $E_b$  is the incident Deuterons energy. Continuous curves show the zero-temperature Astrophysical factor  $S$  for screened (thin curves) and bare (thick curves) nuclei; here we adopted for  $S$  the same expressions of fig. 1 with  $E_{cm} = E_b/2$ . The dashed and dot-dashed thick curves represent the thermal mean with Quantum Uncertainty Effect  $S = \langle \sigma v_{rel} \rangle_{QE} \frac{m_D}{4} \sqrt{\frac{2E_b}{m_D}} \exp\left(\pi \sqrt{\frac{2E_b}{E_b}}\right)$  in KeV b, given by the numerical integration of eq.(3.3); specifically, the dot-dashed curve is relative to the Coulombian  $\sigma_{coll}$ , while the dashed one is plotted for the Ion Sphere Model  $\sigma_{coll}$ , eq. (3.2), with  $\alpha_1 = 1$ .

Debye sphere is too small. The D-H approach needs to be extended to include features that appears as systems leave the weak-coupled regime. Near the weak-coupled regime deviations from the D-H regime can be parameterized by an electron cloud with a steady-state generalized spatial distribution of  $q$ -type (for  $q \rightarrow 1$  electrons are distributed according to a Boltzmann factor): we assume that such deviation can be analytically continued in the strong-coupled regime. Following this strategy, Quarati and Scarfone [30] have recently derived a new screening potential called Modified Debye-Hückel potential using two different approaches. The first one uses a generalized non-linear Poisson or Bernulli equation, the second is based on superstatistics [36, 37]. We discuss this second approach in some detail in the following.

We choose the value  $q = 0$ , also for the Ta matrix, because we can reproduce an electron distribution spatially concentrated around the deuteron, with a strongly depleted tail with cut-off at  $R_{DH}/3$ . We are encouraged in this line of treatment also by the result of ref. [40].

The authors of ref. [30] assumed that non-linear effects produce fluctuations on the inverse Debye-Hückel radius  $1/R_{DH}$ , with a Gamma-function probability distribution:

$$f_q(r, \lambda, \lambda_0) = \frac{A_q(r, \lambda_0)^{\frac{1}{1-q}}}{\Gamma\left(\frac{1}{1-q}\right)} \lambda^{\frac{1}{1-q}-1} e^{-\lambda A_q(r, \lambda_0)}, \text{ where } f_q(r, \lambda, \lambda_0)$$

represents the probability density to observe a certain value  $\lambda$  spreads around a central value  $\lambda_0$ . To obtain from  $f_q(r, \lambda, \lambda_0)$  an electron depleted tail distribution with a cutoff, we limit the

entropic index  $q$  into the  $0 \leq q \leq 1$  interval, assuming:

$$A_q(r, \lambda_0) = \frac{1}{(1-q)g(q)\lambda_0} - r,$$

where  $g(q)$  is a generic entropic index function, that satisfies the condition  $g(1) = 1$  (in ref. [30] the choice  $g(q) = (2-q)^{-1}$  is adopted). The point charge potential  $V_q(r)$  can be identified by the functional:

$$\mathcal{F}_q(r, \lambda_0) = C_q \int_0^\infty f_q(r, \lambda, \lambda_0) e^{-\lambda r} d\lambda,$$

through the relation:

$$rV_q(r) = \frac{D}{C_q \left\langle \frac{1}{R_{DH}} \right\rangle} \mathcal{F}_q(r, \lambda_0), \quad (4.1)$$

where  $C_q = (2-q)g(q)$  is a normalization factor,  $D = Z_1 Z_2 e^2 \left\langle \frac{1}{R_{DH}} \right\rangle$  and  $\lambda_0 = \langle \lambda \rangle = \int_0^\infty f_q(r, \lambda, \lambda_0) \lambda d\lambda = \left\langle \frac{1}{R_{DH}} \right\rangle$ . The charged particles distribution  $\rho(r)$  and the point charge potential  $V_q(r) \propto \rho(r)$  can be derived from eq. (4.1), developing the functional  $\mathcal{F}_q(r, \lambda_0)$  with the previous assumption. A Tsallis cut-off form [38, 39] is obtained for the potential:

$$V_q(r) = \begin{cases} \frac{Z_1 Z_2 e^2}{r} \left( 1 - (1-q)g(q) \left\langle \frac{1}{R_{DH}} \right\rangle r \right)^{\frac{1}{1-q}}, & \text{if } r < \frac{1}{(1-q)g(q) \left\langle \frac{1}{R_{DH}} \right\rangle}, \\ 0 & \text{if } r \geq \frac{1}{(1-q)g(q) \left\langle \frac{1}{R_{DH}} \right\rangle}. \end{cases} \quad (4.2)$$

We note the relation of the power-law expression of  $V_q(r)$  with Tsallis-like distributions. In systems with long-range interactions and correlations and/or memory or in systems that are not in global thermodynamic equilibrium, but rather in a metastable state with a long, finite lifetime, such deformed Tsallis-like distributions are relevant at the very least as convenient parameterizations of deviations from equilibrium; superstatistics is an example of such an approach [36, 37]. The main contribution to the charged particles fusion cross section is given by the screening barrier penetration factor  $P(E)$ . In the standard Debye-Hückel potential case, the simplified expression  $\sigma(E) = \frac{S(E)}{E} P(E)$  can be obtained, that differs from the bare nuclei cross section of eq. (2.3) only for the penetration factor  $P(E) = \exp\left(-\pi\sqrt{\frac{E_G}{E+U_{DH}}}\right)$ , where  $U_{DH} = \frac{Z_1 Z_2 e^2}{R_{DH}}$ . In the case of the modified Debye-Hückel potential  $V_q(r)$ , the penetration factor  $P_q(E)$  is given by the expression:

$$P_q(E) = \exp\left[-\frac{2}{\hbar c} \int_0^{r_q} [2\mu c^2(V_q(r) - E)]^{\frac{1}{2}} dr\right], \quad (4.3)$$

where the classical turning point  $r_q$  has to be determined through the equation  $V_q(r_q) = E$ .

Eq. (4.3) can be analytically solved in the  $q = 0$  case, obtaining  $r_q = Z_1 Z_2 e^2 / (E + g(0)D)$  and  $P_0(E) = \exp\left(-\pi\sqrt{\frac{E_G}{E+g(0)D}}\right)$ .

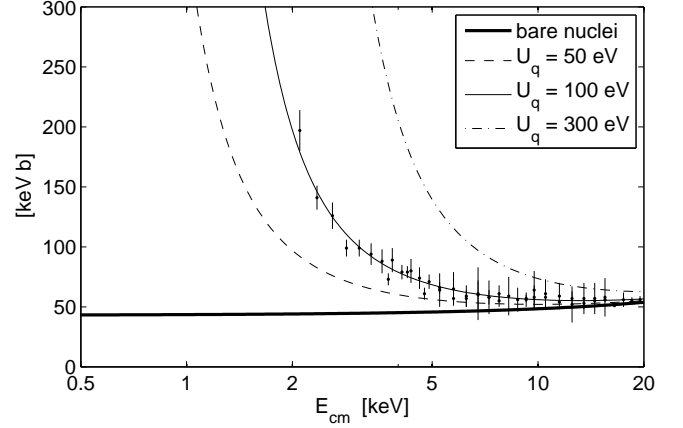


FIG. 3: Astrophysical Factor experimental points from ref. [6]. Bare nuclei curve correspond to  $S_{bare} = 43 + 0.54 E_{cm}$  keV b, while the screened curves are  $S = f_q \cdot S_{bare}(E_{cm})$ , where  $f_q$  is defined in eq.(4.4),  $U_q = e^2 \left\langle \frac{1}{R_{DH}} \right\rangle$ ,  $g(q) = 3 - 2q$  and  $q = 0$ . Ion thermal motion is neglected:  $E_{cm} = E_b/2$ .

The bare nuclei cross section reported in eq. (2.3) can be corrected, to account the modified Debye-Hückel (D-H) screening, multiplying  $\sigma_{bare}(E)$  by the factor

$$f_q = P_q(E) \exp\left(\pi\sqrt{\frac{E_G}{E}}\right) \quad (4.4)$$

For instance we compare the Modified D-H Astrophysical Factor for D+D reaction with the ref. [6] experimental data, adopting the choice  $g(q) = 3 - 2q$ . The results is shown in fig. 3 for the entropic index  $q = 0$ . One can observe as a screening potential  $U_q = D$ , three times lower than in the standard D-H case ( $U_q \sim 100$  eV instead of  $U_{DH} \sim 300$  eV), is required to reproduce the experimental data. An electrostatic screening potential of this order of magnitude has been obtained, for instance, by Saltzmann and Hass [40] through a Thomas-Fermi model of the electron gas in a deuterated-copper target (they obtained a screening potential of 163 eV, instead of the 470 eV needed to reproduce the experimental results).

Now we are treating  $g(q)$  and  $q$  as free parameters, but, in principle, a link can be establish between the inverse D-H Radius, the temperature fluctuations and the  $q$ -index:  $\frac{\Delta\left(\frac{1}{R_{DH}}\right)}{\frac{1}{R_{DH}}} = \frac{\Delta(k_b T)}{k_b T} = \sqrt{1-q}$  and by the electron charge  $q$ -distribution around the ion (if experimentally known or as deduced from a model). By this way the modified Debye-Hückel potential can be obtained starting from the environment condition.

## 5. CONCLUSION

We studied two effects of non-Maxwellian velocity distributions in plasmas as possible explanations for the fusion rate enhancements observed in deuterated-metal target experiments: modifications to the thermal mean  $\langle \sigma v_{rel} \rangle$  due to the

Quantum Uncertainty Effect and the stronger screening arising from non-thermal electron distributions. Either effect reduces the discrepancy between theoretical models and experimental results.

The broadening of the momentum distribution due to the QE has been studied using a collisional cross section  $\sigma_{coll}$  derived by the Ion Sphere Model, eq. (3.2), model that captures the main features of collisions in the strong coupled plasmas that characterize the experimental environment.

We have been able to obtain a rate enhancement up to energy thresholds much higher than previous calculations [27] and even above the one observed in experiments, as shown in fig. 2. If one makes the reasonable additional hypothesis that only a fraction of the absorbed deuterons are in a quasi-free plasma-state, which can be shown to be still strongly coupled, one should be able to reproduce the experimental behavior.

We intend to explore more quantitatively this possibility in the near future.

We have also considered the effects of plasma screening on the reaction cross sections, when the modified Debye-Hückel potential introduced by Quarati and Scarfone in ref. [30] is used. Already in ref. [40] a screening potential  $U_e \sim 100$  eV was obtained, greater than the adiabatic limit  $U_{ad}$ , but still too low to reproduce the experimental results. In this work we showed that the modified D-H potential of eq. (4.2), with an appropriate choice of the function  $g(q)$  and of the entropic index  $q$ , can reproduce the data, see in fig. 3. In principle the value of the entropic index  $q$  can be derived from the plasma equation of state and  $g(q)$  from the electron charge distribution around the ion, then the modified D-H screening contribution to the rate enhancement can be evaluated without free parameters. We shall investigate this last point in a future work.

- 
- [1] H. Yuki, J. Kasagi, A.G. Lipson, T. Ohtsuki, T. Baba, and T. Noda, *JETP Lett.* **68**, 823 (1998).
  - [2] J. Kasagi et al. *J. phys. soc. Jpn.* **71**, 2881 (2002).
  - [3] K. Czerski, A. Huke, A. Biller, P. Heide, M. Oeft and G. Ruprecht, *Europhys. Lett.* **54**, 449 (2001).
  - [4] A. Huke, K. Czerski and P. Heide, *Nucl. Instrum. Methods. B* **256**, 599 (2007), [arXiv:nucl-ex/0701065].
  - [5] A. Huke, K. Czerski, P. Heide, G. Ruprecht, N. Targosz and W. Zebrowski, *Phys. Rev. C* **78**, 015803 (2008), [arXiv:nucl-ex/08054538].
  - [6] F. Raiola et al., *Eur. Phys. J. A* **13**, 377 (2002).
  - [7] F. Raiola et al., *Phys. Lett. B* **547**, 193 (2002).
  - [8] C. Bonomo et al., *Nucl. Phys. A* **719**, 37c (2003).
  - [9] F. Raiola et al., *Eur. Phys. J. A* **19**, 283 (2004).
  - [10] F. Raiola et al., *J. Phys. G Nucl. Partic.* **31**, 1141 (2005).
  - [11] F. Raiola et al., *Eur. Phys. J. A* **27**, 79 (2006).
  - [12] J. Kasagi et al. *J. phys. soc. Jpn.* **73**, 608 (2004).
  - [13] J. Kasagi, *Prog. Theor. Phys. Supp.* **154**, 365 (2004).
  - [14] J. Cruz et al., *Phys. Lett. B* **624**, 181 (2005).
  - [15] J. Cruz et al., *J. Phys. G Nucl. Partic.* **35**, 014004 (2008).
  - [16] E. Salpeter, H. Van Horn, *Astrophys. J.* **155**, 183 (1969); A. Alastney, B. Jancovici, *Astrophys. J.* **226**, 1034 (1978); M. Baus, J. P. Hansen, *Phys. Rep.* **59**, 1 (1980); L. Bracci, V. Melezhik, G. Fiorentini, G. Mezzorani, P. Quarati, *Nucl. Phys. A* **513**, 316 (1990).
  - [17] S. Ichimaru, *Statistical plasma physics Vol I*, (Addison-Wesley, USA 1992).
  - [18] G. Fiorentini, C. Rolfs, F. L. Villante and B. Ricci, *Phys. Rev. C* **67**, 014603 (2003) [arXiv:astro-ph/0210537].
  - [19] M. Coraddu, M. Lissia, G. Mezzorani, Y. V. Petrushevich, P. Quarati and A. N. Starostin, *Physica A* **340**, 490 (2004) [arXiv:nucl-th/0401043].
  - [20] V. M. Galitskii and V. V. Yakimets, *JETP* **24**, 637 (1967).
  - [21] M. Coraddu, G. Kaniadakis, A. Lavagno, M. Lissia, G. Mezzorani and P. Quarati, *Braz. J. Phys.* **29**, 153 (1999) [arXiv:nucl-th/9811081].
  - [22] A. N. Starostin, V. I. Savchenko, and N. J. Fisch, *Phys. Lett. A* **274**, 64 (2000).
  - [23] A. N. Starostin, A. B. Mironov, N. L. Aleksandrov, J. N. Fisch, and R. M. Kulrud, *Physica A* **305**, 287 (2002).
  - [24] A. V. Eletskii, A. N. Starostin, and M. D. Taran, *Phys. Usp.* **48**, 281 (2005).
  - [25] M. Lissia and P. Quarati, *Europhys. Lett.* **36**, 211 (2005) [arXiv:astro-ph/0511430].
  - [26] V. Petrushevich, P. Quarati and A. N. Starostin, *Physica A* **340**, 496 (2004) [arXiv:nucl-th/0402025].
  - [27] M. Coraddu, M. Lissia, G. Mezzorani and P. Quarati, *Eur. Phys. J. B* **50**, 11 (2006) [arXiv:nucl-th/0512066].
  - [28] Y.E. Kim and A.L. Zubarev, *Jpn. J. Appl. Phys.* **45**, 552 (2006)
  - [29] Y.E. Kim and A.L. Zubarev, *Jpn. J. Appl. Phys.* **45**, 552 (2006)
  - [30] P. Quarati, A.M. Scarfone, *Astrophys. J.* **666**, 1303 (2007), [arXiv:astro-ph:07053545].
  - [31] H. Andersen and J.F. Ziegler, *The Stopping and Ranges of Ions in Matter* (Pergamon, New York, 1977 and SRIM 2008).
  - [32] A. Huke, K. Czerski, S.M. Chun, A. Biller and P. Heide, *Eur. Phys. J. A* **35**, 243 (2008), [arXiv:nucl-th/08031071].
  - [33] F. Ferro and P. Quarati, *Phys. Rev. E* **71**, 026408 (2008)
  - [34] S. Ichimaru, *Rev. Mod. Phys.* **54**, 1017 (1982)
  - [35] S. Ichimaru, *Rev. Mod. Phys.* **65**, 255 (1993)
  - [36] C. Beck, *Phys. Rev. Lett.* **87**, 180601 (2001).
  - [37] C. Beck, *Continuum. Mech. Therm.* **16**, 293 (2004).
  - [38] C. Tsallis, *J. Stat. Phys.* **52**, 479 (1988).
  - [39] C. Tsallis and E. P. Borges, *Application to nuclear and high energy physics, Proceedings of correlations and Fluctuation in QCD*, (World Scientific, Singapore 2003), [arXiv:cond-mat:0301521].
  - [40] D. Saltzman and M. Hass, *Eur. Phys. J. A* **38**, 359 (2008), [arXiv:nucl-ex:08060218].